

## Impurity analysis using a space resolved transmission grating based imaging spectrometer on NSTX

D. Kumar<sup>1</sup>, D. Stutman<sup>1</sup>, R. E. Bell<sup>2</sup>, M. Finkenthal<sup>1</sup>, D. J. Clayton<sup>1</sup>, K. Tritz<sup>1</sup>  
 B. P. LeBlanc<sup>2</sup>, A. Diallo<sup>2</sup>, M. Podesta<sup>2</sup>

<sup>1</sup>*The Johns Hopkins University, Baltimore, USA.*

<sup>2</sup>*Princeton University, Princeton, USA.*

Measurement of the impurity content and transport is critical for fusion experiments. The plasma spectroscopy group at the Johns Hopkins University is developing an impurity diagnostic package consisting of two complimentary diagnostics - (a) Multi-energy filtered SXR arrays (ME-SXR) measure the plasma emission with high space and time resolution but with coarse energy discrimination[1], (b) A transmission grating imaging spectrometer (TGIS) measures the EUV impurity line emission with lower time resolution but higher energy resolution[2]. The space resolved TGIS spectra determine the impurity fractions needed for modeling the ME-SXR data and also for standalone impurity monitoring. This paper briefly describes the application of the TGIS for diagnosing the impurity fractions on NSTX.

The basic layout of the TGIS is shown in Fig. 1. The detailed design of the TGIS has been published earlier[2].

The device uses a CsI coated MCP image intensifier as a 2-D detector. The wavelength coverage is 30-700 Å and the spectral resolution around 10 Å. The time resolution of the instrument is limited by a slow image acquisition rate of 3 frames/s. The TGIS has a tangential midplane view covering the region from  $r/a \sim 1$  to the magnetic axis with spatial resolution around  $a/15$ . The field of view of TGIS includes the region where the heating beams enter the plasma, thus enabling measurement of both fully stripped low-Z impurities through their CX excited emission and higher-Z impurities through their electron excited emission.

The wavelength and spatial calibration of the instrument was performed on a table top spatially extended Penning Ionization Discharge (PID) source. The brightness of the EUV emission lines from the PID are comparable to the brightness measured on NSTX. The diffraction effi-

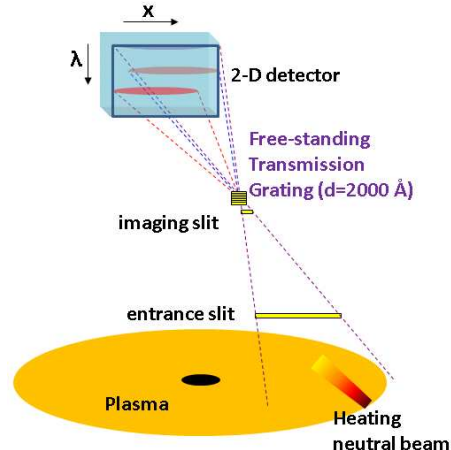


Figure 1: Principle of operation of TGIS. The two slits define a narrow fan beam which is diffracted by the free standing transmission grating. The aperture of the grating determines the spatial resolution of the instrument.

ciency of the EUV grating was calibrated at the Synchrotron Ultraviolet Radiation Facility at NIST[2]. The results show nearly constant efficiency of around 10% , between 100 Å to 300 Å.

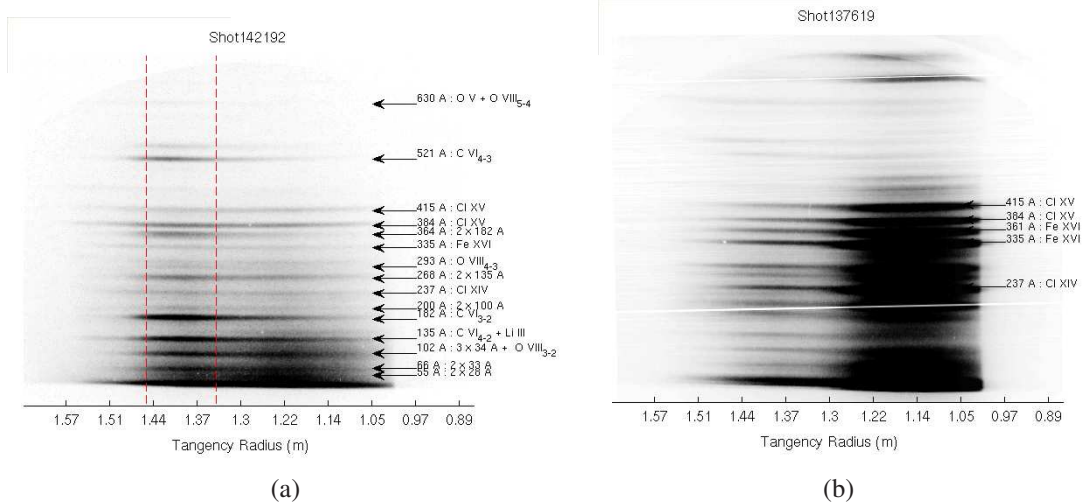


Figure 2: (a) TGIS spectrum from neutral beam heated plasma shot on NSTX. The charge exchange radiation peaks in the region of intense beam interaction contained within dotted red lines. The transitions of charge exchange lines are listed in the subscripts. (b) TGIS spectrum from neutral beam heated plasma shot on NSTX with iron and chlorine accumulation in the core. The intensity decrease for  $R > 1.2$  m is an artifact due to vignetting of the field of view.

The instrument was operated throughout the 2010 NSTX campaign without any adverse effect from the intensive Li wall conditioning. The space resolved TGIS spectrum from a typical neutral beam heated plasma is shown in Fig. 2(a). The core plasma parameters for the spectra shown in Fig. 2(a) are  $T_e \sim 0.9$  keV and  $n_e \sim 7 \times 10^{13} \text{ cm}^{-3}$ . The space resolving capability of the instrument is elucidated by the fact that charge exchange spectral lines in Fig. 2(a) are localized to the beam interaction region, while the electron excited emission from Li- and Be-like Cl extends all the way into the core.

A few plasma shots had impurity accumulation and significant radiation from the core of the plasma. Accumulation of Cl and Fe in the core is clearly visible from the space resolved TGIS spectrum shown from one such shot in Fig. 2(b). In contrast, the spectra from Ohmic heated shots consists of edge emission from C, O and Li[2]. The spectra of RF heated plasmas show the presence of Na- like Cu all the way into the core, whenever arcing occurred in the RF antennas.

The  $n(C^{6+})$  density calculated by an absolutely calibrated visible charge exchange spectroscopy system using the C VI n=8-7 line[3], and the known charge exchange cross sections[4] were used to simulate the brightness of the C VI n=3-2 line. The simulated brightness of C VI n=3-2 charge exchange line was used as a reference for estimating the absolute photon calibration of TGIS. The comparison of the simulated and measured brightness profiles of the charge

exchange radiation show good agreement (see Fig. 3).

For non-resonant transitions in the EUV range, the contribution from the collisional electron excitation is negligible compared to the charge exchange from heating neutral beams. Thus, comparison of charge exchange brightness from low Z impurities (like O and N) yield their respective densities. Typical oxygen concentrations in NSTX were found to be  $\sim 5 \times 10^{-3} \times n_e$ .

The fractions of medium-Z impurities such as Cl or Fe were determined in a more approximate manner using a coronal equilibrium collisional excitation model that did not include transport or thermal charge exchange from edge neutrals. The typical chlorine concentrations in NSTX were  $\gtrsim 10^{-4} \times n_e$ , and Fe was either not detected or present in extremely low concentrations  $\lesssim 10^{-5} \times n_e$ .

The impurity fractions determined by the TGIS helped model the ME-SXR emissivity profiles in the region between  $1 < r/a < 0.6$ , which is generally difficult in NSTX due to the sub-keV electron temperatures and the presence of a mixture of low- and medium-Z impurities[1].

Several important improvements are possible for the TGIS device. Perhaps the most important improvement is increasing the image readout speed. An f/0.95 objective was used to couple the image of the spectrum from the MCP intensifier to a camera (Allied Vision Prosilica GC1380H). The high sensitivity and readout capability of the camera enables high time resolution of  $\sim 10$  ms. Fig. 4 shows a typical spectrum obtained by the fast readout system on the PID source with Al electrodes and Ne gas.

Experiments on the PID and NSTX also showed that the TGIS is sensitive enough to allow decreasing the slit widths and the grating aperture, in order to increase the spectral and spatial resolution. The TGIS planned for 2011-12 NSTX campaign will have  $\sim 6 \text{ \AA}$  spectral resolution,  $\sim 1 \text{ cm} (\sim 0.5^\circ)$  spatial resolution, and high time resolution ( $\gtrsim 10$  ms). In addition to the ability to monitor transient impurity fluxes, these enhancements open up the possibility of using the TGIS for perturbative impurity transport measurements, from the edge to the core plasma.

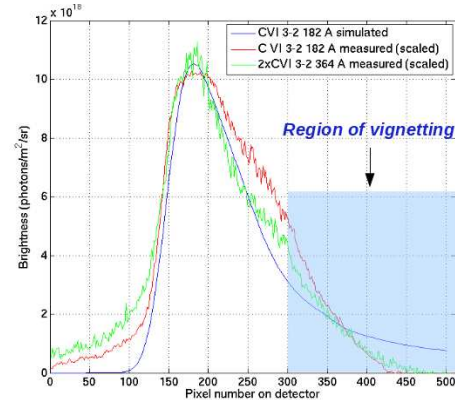


Figure 3: Comparison of brightness profiles of the simulated and measured charge exchange radiation from C VI n=3-2 line.

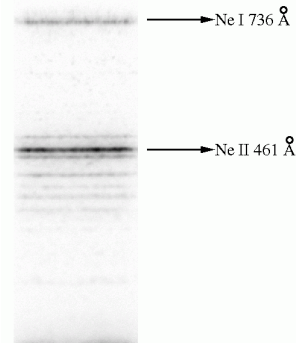


Figure 4: 10 ms exposure spectrum with higher spatial ( $0.5^\circ$ ) and wavelength (6 – 7  $\text{\AA}$ ) resolution obtained by the TGIS on a PID.

Mo tiles have been installed on the inner divertor of NSTX for the 2011-12 experimental campaign. M-shell radiation around 75 Å is expected to be dominant from Mo ions in the core of NSTX plasmas with electron temperatures around 1 keV [5]. As can be noted from Fig. 2(a), this wavelength range is polluted by the second order Carbon Ly- $\alpha$  emission. Thus, in order to facilitate detection of Mo radiation, a 1  $\mu$ m thick Parylene-N filter manufactured by the Lebow Company has been installed inside the TGIS. One half of the spectrum is observed through the filter, which severely attenuates Carbon Ly- $\alpha$  emission, but transmits Mo emission.

Another significant upgrade to the TGIS involves replacing the MCP detector with an EUV direct photon detection CCD camera. Direct detection XUV CCDs have high quantum efficiency over a broad spectral range ( $> 15 - 20\%$  from a few eV to a few keV), fast readouts and flexible binning capability. Such cameras (for example Princeton Instrument's PIXIS XO series) have been used on experiments like NSTX, and have shown significant resistance to neutron and radiation fields. A high wavelength resolution ( $\sim 4 \text{ \AA}$ ) spectrum obtained by a TGIS using an ANDOR IKON-M 934 [DO] camera having a back illuminated sensor is shown in Fig. 5. A similar TGIS equipped with a PIXIS XO 400B camera is being designed for W spectroscopy and transport experiments on the FTU tokamak. This work is motivated by preliminary results on FTU and NSTX which show that the few Å spectral resolution of the TGIS combined with its space resolving ability make it an ideal instrument for W spectroscopy in the 20-800 Å range, where spectra are dominated by broad unresolved features and are difficult to interpret in terms of emitting charge states without space resolved measurements.

*The work at Johns Hopkins University was supported under US DOE Grants Numbers DE-FGO2-86ER53214 and DE-S0000787. The work at PPPL was supported under US DOE Contract Number DE-AC02-09CH11466.*

## References

- [1] D. J. Clayton *et al*, in these proceedings.
- [2] D. Kumar *et al*, Rev. Sci. Instrum., **81**(10):10E507, 2010.
- [3] R. E. Bell and R. Feder, Rev. Sci. Instrum., **81**(10):10D724, 2010.
- [4] R. C. Isler, Plasma Phys. Controlled Fusion, **36**(2):171, 1994.
- [5] M. Finkenthal *et al*, J. Phys. B: At. Mol. Phys., **18**(22):4393, 1985.

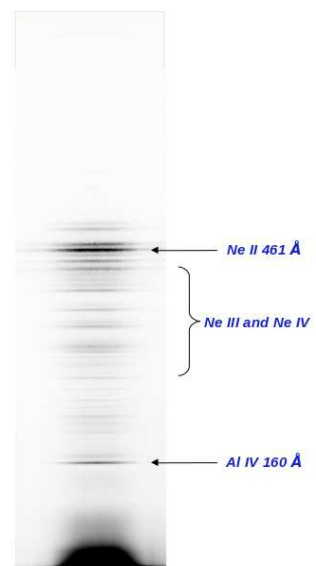


Figure 5: Higher resolution (4 Å) spectra obtained using direct EUV photon detection CCD camera.